Int. J. Electrochem. Sci., 9 **(2014)** 8189 - 8198

International Journal of
ELECTROCHEMICAL
SCIENCE
www.electrochemsci.org

Synthesis and Characterization of Cu@Cu_2O Core Shell Nanoparticles Prepared in Seaweed *Kappaphycus alvarezii* Media

Hajar Khanehzaei[1], *Mansor B Ahmad*[1,*], *Kamyar Shameli*[1,*], *Zahra Ajdari*[2]

[1] Department of Chemistry, Faculty of Science, Universiti Putra Malaysia, 43400 UPM Serdang, Selangor, Malaysia
[2] Innovation Center for Confectionery Technology (MANIS), Faculty of Science and Technology, Universiti Kebangsaan Malaysia, 43600 Bangi, Selangor Darul Ehsan, Malaysia
[*]E-mail: mansorahmad@gmail.com, kamyarshameli@gmail.com

Received: 14 August 2014 / *Accepted:* 29 September 2014 / *Published:* 28 October 2014

This study reports a synthesis of Cu@Cu_2O core shell nanoparticles (NPs) in *Kappaphycus alvarezii* (*K. alvarezii*) media via a chemical reduction method. The nanoparticles were synthesis in an aqueous solution in presence of *K. alvarezii* as stabilizer and $CuSO_4.5H_2O$ precursor. The synthesis proceeded with addition of NaOH as pH moderator, ascorbic acid as antioxidant and hydrazinium hydroxide as the reducing agent. The resulting nanoparticles characterized by using UV–vis spectrum, X-ray diffraction, Transmission electron microscopy, Fourier transform infrared (FT-IR) and atomic force absorption (AFM). The UV-visible spectra indicate to peaks at 590 nm and 390 which confirmed the formation of Cu@Cu_2O-NPs. The XRD used in analysis of the crystal structure of nanoparticles. The morphology and structure of the *K. alvarezii*/Cu@Cu_2O-NPs were investigated by TEM and AFM. The average size of Cu@Cu_2O-NPs obtained were around 53 nm that confirmed by using X-ray diffraction, TEM and AFM. The Fourier transform infrared (FT-IR) spectrum suggested the complexation present between *K. alvarezii* and Cu@Cu_2O-NPs.

Keywords: *Kappaphycus alvarezii*, copper nanoparticles, seaweed, copper (I) oxide, core shell nanoparticles, zeta potential.

1. INTRODUCTION

Nanoparticles have been extensively studied in the last decade because of their high surface to-volume ratios and their potential applications in magnetic recording [1–5], catalysis [6, 7] or medical diagnosis or treatments [8–11]. There are many types of nanoparticles for various applications, such as

metallic, Non-metallic, oxide nanoparticles. Metallic nanoparticles have attracted due to their desirable properties and new applications compared with bulk ones [12–15].

Among metal nanoparticles, copper nanoparticles have recently attracted increased attention because of their low cost (in contrast to Au and Ag) and novel optical, catalytic, mechanical, electrical, magnetic, and heat conduction properties [16]. There are different methods of synthesis of Cu-NPs including polyol process [17], metal vapour synthesis [18], laser ablation [19], micro-emulsion techniques [20] and thermal reduction [21] cuprous oxide (Cu_2O) is a well-known material in the history of semiconductor. The Cu_2O nano-materials are very potential as p-type semiconductor with unique optical and magnetic properties, easy accessibility and low toxicity [22]. At present, the Cu_2O nanoparticles (NPs) are prepared by such methods as microwave irradiation [23] and liquid phase reducing [24] sol–gel [25] and electrochemistry [26].

Metal core-shell nanoparticles (NPs) as a semiconductor have attracted many interests due to their potential application in many areas and also interesting physics involved in the process. Copper oxide (CuO and Cu_2O) compounds are interesting materials because of their application as catalysts, antibacterials, interconnects in electronic, corrosion of alloys, etc [27]. The surfaces of copper oxide can react with gases or solutions and can behave as a catalyst or a gas sensor. However many surface properties of copper oxides are not well understood. The identification of the actual oxidation state of copper in the core shell system is critical to understand their chemical behaviour. Almost all of the core-shell nanoparticles fabrications are based on wet chemical methods [28].

The *K. alvarezii* economically important red tropical seaweed, which is highly demanded for its cell wall polysaccharide, is the most important source of kappa carrageenan. It is easily accessible, in huge amounts, for food and pharmaceutical applications [29]. The kappa carrageenan comprises a family of linear water-soluble sulphated polysaccharides with an alternating backbone consisting of α (1–4)-3, 6-anhydro-D-galactose and β (1–3)-D-galactose extracted from red seaweeds [30, 25]. The kappa carrageenan has one sulphate group for every 2-sugar units with a 25% of sulphate content approximated [25]. Due to their biocompatibility and ability to form hydrogels; carrageenan has been extensively used as gelling agent in food and pharmaceutical industries. The bio-route of synthesizing metal nanoparticles is the best approach for their biological examinations [30, 26].

This research reports a simple synthesis of Cu@Cu_2O-NPs via a chemical method with *K. alvarezii*, hydrazinium hydroxide as the Reducing agent and ascorbic acid as antioxidant.

2. EXPERIMENTAL SECTION

2.1. Materials

All reagents in this work were of used as received without further purification. The $CuSO_4.5H_2O$ (99 %) was used as the copper precursor and obtained from Hamburg Chemical GmbH, ascorbic acid (90 %) was obtained from Sigma Aldrich while hydrazinium hydroxide (about 100 % N_2H_5) and NaOH were obtained 99 % from MERCK, Germany and a raw seaweed *Kappaphycus alvarezii* was obtained from Sabah, Malaysia. All solutions were freshly prepared using double distilled water.

2.2. Preparation of Aqueous Solution of K. alvarezii

Firstly, the seaweed washed under running water to remove salt, dirt and foreign particles. It then was soaked overnight (24 h) in distilled water to bleach the yellowish colour from the seaweed, so it became colourless. After that, the sample was rinsed and dried under sunlight for 3 days. Afterward, the dried seaweed was chopped into small pieces before being blended using a hammer mill with 3 mm filter diameter. Finally, this product was stored until further processing. The dried seaweed reduced the storage space required and can be stored for a number of years without appreciable loss of the gelling property. Finally to prepare aqueous solution (0.2 g) of this sample dissolved in (40 mL) double distilled water by heating and stirring.

2.3. Synthesis of Cu@Cu_2O-NPs in K. alvarezii Media

Copper nanoparticles were synthesized by the method which used by Usman et al [25]. For synthesis of Cu-NPs (0.4 g) of $CuSO_4.5H_2O$ in (10 mL) double distilled water, than the mediated blue coloured aqueous solution was then added to solution of *K. alvarezii* while the colour changed from blue to light blue. After stirring and refluxing at 120 °C for 20 min, 2.0 mL of NaOH (0.6 M) was added to the solution while the solution. After 20 min, a light green colour was observed. Adding hydrazinium hydroxide was followed with give a quick yellowish brown which changed to deep red after few min stirring. The solution was stirred for 20 min. The suspensions were finally centrifuged, washed three times with double distil water and kept in stove at 60 °C.

2.4. Characterization Methods and Instruments

The powder X-ray diffraction (PXRD) with Cu Kα radiation was used to measure the crystallinity of sample. TEM observations were performed with a Hitachi (Tokyo, Japan) H-7100 electron microscope, and particle size distributions were determined by use of UTHSCSA Image Tool software, Version 3.00. The SPR of the sample was determined using a UV 1650 PC-Shimadzu B UV-visible spectrophometer (Shimadzu, Osaka, Japan). Moreover, the FT-IR spectra were recorded over the range of 200-4000 cm^{-1} utilizing the Series 100 PerkinElmer FT-IR 1650 spectrophotometer. Atomic force absorption (AFM) was used to measure the morphology and size of produced particles. The AFM observations were carried out using AFM model Q-Scope 350. After the reactions, the sample was centrifuged by using a high-speed centrifuge machine (Avanti J25, Beckman). The zeta potential measurements were also performed using a Zeta sizer Nano-ZS (Malvern Instruments, Worcestershire, UK).

3. RESULTS AND DISCUSSION

The results indicate that the Cu@Cu_2O-NPs could be obtained using hydrazinium hydroxide as reducing agent, *K. alvarezii* as the capping agent, NaOH as the pH moderator and ascorbic acid as the

antioxidant in the solution. Figure 1 demonstrates a series colour changes during the preparation of Cu@Cu_2O-NPs. These colour changes are due to the chemical reactions taking place. The *K. alvarezii* copper ions complex [Figure 1(a)] is light blue which is resulted from addition of Cu ions solution to *K. alvarezii* solution. To prevent the obtained NPs from more oxidation, ascorbic acid was added at this stage that no colour change was observed after this addition. After addition of NaOH a light green [Figure 1(b)] colour was observed. The UV-visible analysis of sample at this stage did not indicate any surface plasmon resonance peak, which shows that the NaOH added could not reduce the Cu^{2+} in K. *alvarezii* to Cu or Cu_2O-NPs.

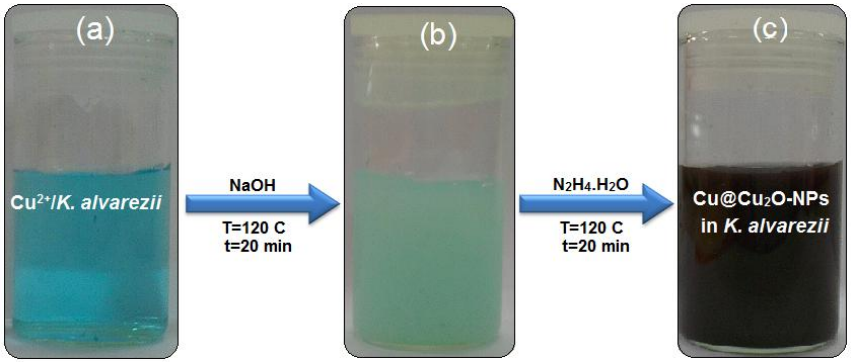

Figure 1. Photographs of the sample at different stage of synthesis indicating colour changes.

Finally the Cu@Cu_2O-NPs was formed following the addition of hydrazinium hydroxide with a quick brick red colour which changed dark brownish-red [Figure 1(c)]. More over the observation of two colours after addition of hydrazinium hydroxide (a quick brick red colour which changed dark brownish-red) suggests that Cu@Cu_2O-NPs formed in two steps which include the formation of Cu-NPs in first and second step is oxidation of Cu-NPs and forms a layer of Cu_2O over Cu particle surface. The UV-visible analysis of sample was corroborated the preparation of Cu@Cu_2O-NPs.

3.1. UV-visible Spectroscopy Analysis

Figure 2a, indicates the UV-visible absorption spectra of *K. alvarezii*/Cu^{2+} complex. Figure 2b shows the UV-visible absorption spectra of the Cu@Cu_2O-NPs in aqueous solution. The absorption peaks due to the surface plasmon resonance (SPR) of Cu@Cu_2O-NPs colloids were observed at 590 nm and 390 which attributed the preparation of Cu@Cu_2O-NPs. Due to the surface plasmon resonance effect, the Cu-NPs typically display absorption in the range of 500-600 nm [31, 32] and the Cu_2O-NPs show absorption in the range of 300-500 nm [33, 34]. As shown in Figure 2b the SPR peak at 590 nm which is correspond to the Cu-NPs have higher intensity compared to the SPR peak at 390 nm. It is suggests that the ratio of Cu-NPs is more than ratio of Cu_2O-NPs in the contain of *K. alvarezii*/Cu@Cu_2O-NPs. Peak appearing after adding hydrazinium hydroxide implies that NPs were not formed after addition of NaOH.

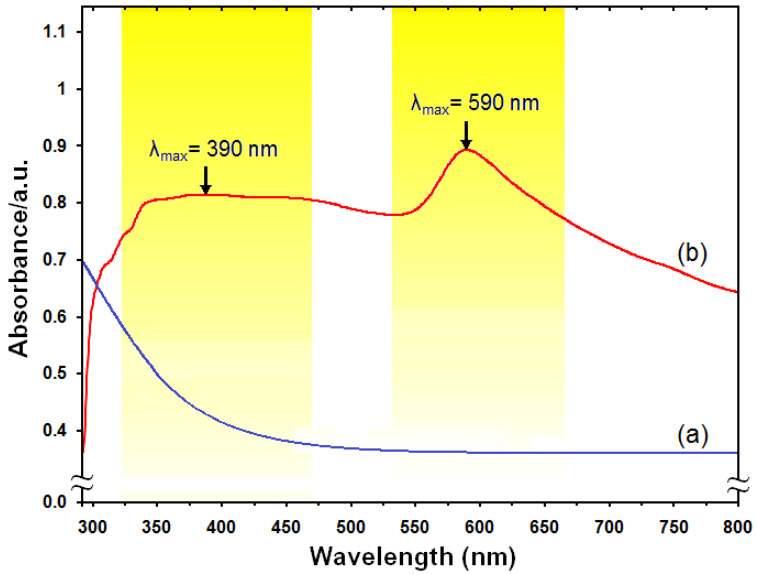

Figure 2. UV-visible absorption of *K. alvarezii*/Cu^{2+} complex (a) and Cu@Cu_2O core shell in *K. alvarezii* media (b).

3.2. X-ray Diffractometry

As shown in Figure 3 the ratio of Cu and Cu_2O-NPs in the sample is 75% and 25%, respectively and the ratio of Cu@Cu_2O-NPs are in accordance with the UV-visible spectral results. The comparison between the PXRD patterns of the *K. alvarezii* and *K. alvarezii*/Cu@Cu_2O-NPs in the angle range of 2θ (5–90) indicated the formation of the intercalated Cu@Cu_2O nanostructure [Figure 3(a–b)]. The broad diffraction peak, which was centered at 21.51°, is attributed to *K. alvarezii* (Figure 3a). The peak values are located at 43.09°, 50.32° and 74.07°, (Figure 3b) which correspond to the miller indices (111), (200) and (220), respectively and represent face centered cubic (fcc) crystal structure of Cu-NPs [31].

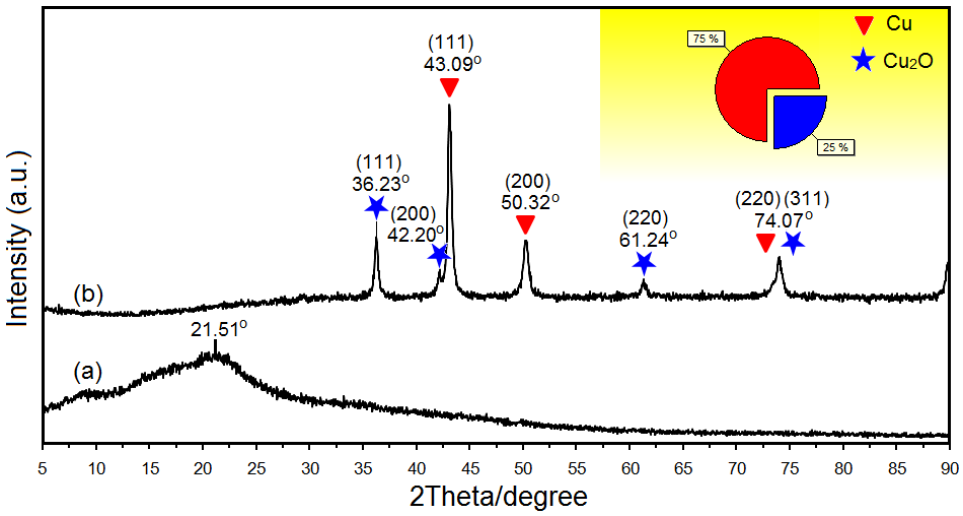

Figure 3. XRD peaks of *K. alvarezii* (a) and Cu@Cu_2O-NPs core shell in *K. alvarezii* media (b).

The diffraction angels observed at 36.23°, 42.20°, 61.24° and 74.07° (Figure 3b) are relevant to Cu_2O. The particles size can be calculated using Scherer's Equation (1):

$$n=k\lambda/\beta \cos \theta \quad (1)$$

Where K is the Scherer's constant with value from 0.9 to 1 (shape factor), where λ the X-ray wavelength (1.5418 Å), β1/2 is the width of the XRD peak at half height and θ is the Bragg angle [9]. The size of obtained nanoparticles is around 53 nm.

3.3. Transmission Electron Microscopy

Figure 4 demonstrates the TEM images and size distribution and calculated histogram of *K. alvarezii*/Cu@Cu_2O-NPs. The TEM images and their size distributions showed that the mean diameters and standard deviation of Cu@Cu_2O-NPs were about 52.99±18.64 nm. The number of Cu@Cu_2O-NPs counted in the TEM images was around 60 nm. The distribution of Cuo@Cu_2O-NPs in TEM images are in accordance with the UV-vis spectral study. In addition, the TEM image clearly shows the core-shell structure of produced nanoparticles.

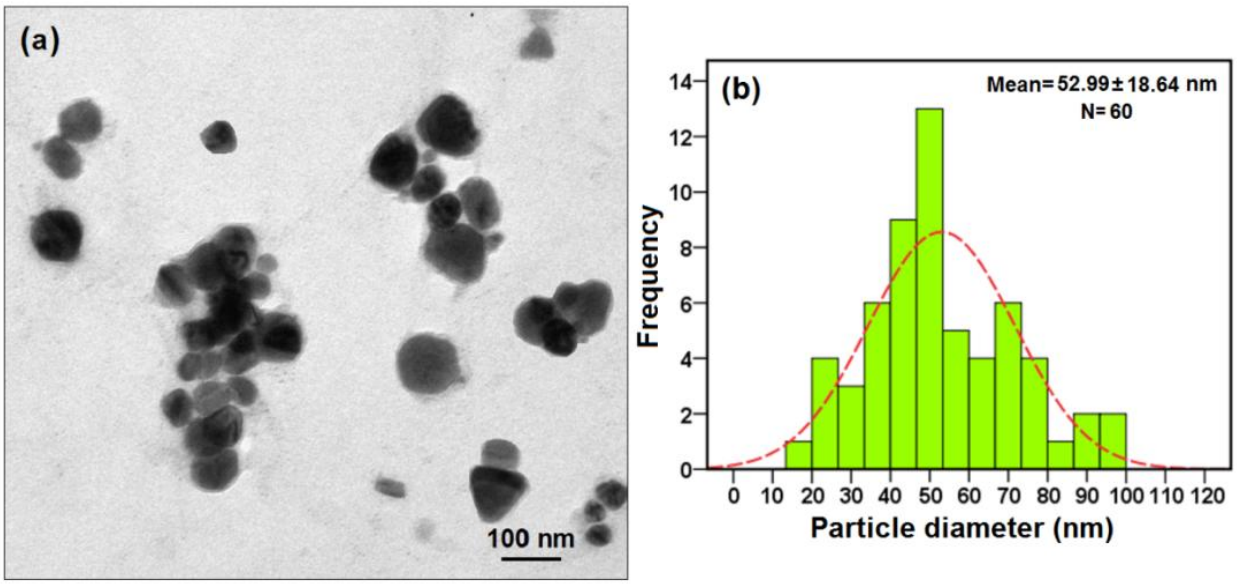

Figure 4. Transmission electron micrographs and particle size distribution of *K. alvarezii*/Cu@Cu_2O-NPs.

3.4. Atomic Force Microscope

The *K. alvarezii*/Cu@Cu_2O-NPs was characterized by atomic force microscopy (AFM) for its detail size and morphology of *K. alvarezii*/Cu@Cu_2O-NPs. The AFM images resultant *K. alvarezii* and *K. alvarezii*/Cu@Cu_2O-NPs were observed as amorphous and spherical in shapes shown in Figure 5 (a-b). There have been reported that the topographical images of irregular shape for *K. alvarezii* and regular shape for Cu@Cu_2O-NPs have documented. The fabrication of nanoparticles were imaged by AFM to understand the exact configuration of the fabricated nanoparticles and also used to verify that

the nanoparticles were more or less homogenous in size and were spherical in shape. The particles size of the Cu@Cu_2O-NPs ranged in the size estimated from 40 to 70 nm and can be controlled by varying the synthesis condition. The size of Cu@Cu_2O-NPs in the range of ≤ 60 was estimated using the *Debye Scherrer* equation with data obtained from XRD [35, 36].

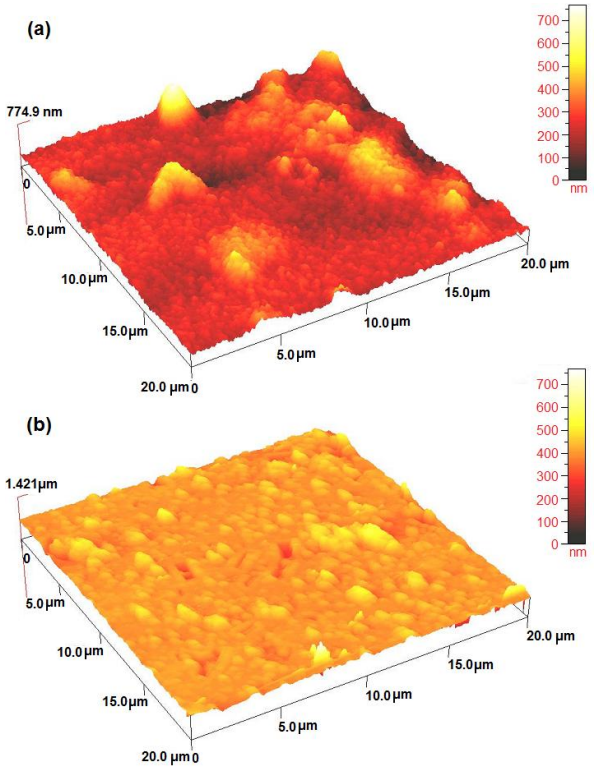

Figure 5. The atomic force microscope image of *K. alvarezii* (a) and *K.alvarezii*/Cu@Cu_2O-NPs (b).

3.5. FT-IR Chemical Analysis

Figure 6 shows the FT-IR spectra of *K. alvarezii* and *K. alvarezii*/Cu@Cu_2O-NPs. In the FT-IR spectrum of *K. alvarezii* (Figure 6a), the absorption peaks at 3366 cm^{-1} and 2919 cm^{-1} are ascribed to stretching vibrations of -OH and C-H groups, respectively [25]. The absorption band at 1638 is attributed to the polymer bound water. The peak at 1410 cm^{-1} is corresponds to the sulphate stretching. The peak at 1361 cm^{-1} is assigned to methylene group bending. The peak at 1410 cm^{-1} is corresponds to the sulphate stretching. The peak at 1361 cm^{-1} is assigned to methylene group bending. The absorption band in 1213 cm^{-1} originate from O=S=O asymmetric stretching. The two peaks at 1146, 1122 cm^{-1} are attribute S=O and C-O-C asymmetric stretching respectively. The intense band in 1020 cm^{-1} is representing glycosidic linkage. The band at 917 cm^{-1} is associated with C-O-C stretching vibration of 3, 6-anhydro bridges. The band at 837 cm^{-1} is due to C4-O-S stretching in β-D-galactose. The peaks at 692, 565 and 350 cm^{-1} are assigned to S=O=S bending [37].

The comparison between FT-IR spectra of *K. alvarezii* (Figure 6a) and *K. alvarezii*/Cu@Cu_2O-NPs with core shell structure shows that the absorption peaks at 3366, 2919 and 1638 cm^{-1} are disappeared (Figure 6b). Moreover, the intensity of two peaks at 1410 and 1361 cm^{-1} were reduced. In

addition, the new peaks at 689 and 304 cm^{-1} representing Cu@Cu_2O nanoparticles [22]. These results confirm that the Cu@Cu_2O-NPs surface capped by the internal lone pair oxygen atoms, some hydroxyl and sulphates groups of the polymer.

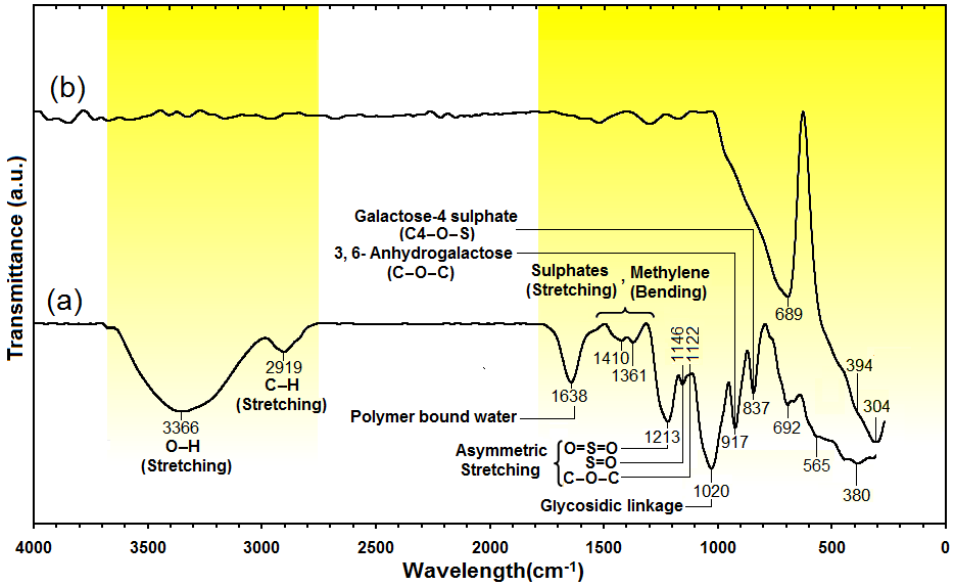

Figure 6. FT-IR spectra of *K. alvarezii* (a) and *K. alvarezii*/Cu@Cu_2O-NPs (b).

3.6. Zeta potential measurement

The stability of the *K. alvarezii*/Cu@Cu_2O-NPs was determined by measurement of zeta potential. As shown in the Figure 7, the Cu@Cu_2O-NPs obtained possesses a negative zeta potential value. A minimum of ±30 mV zeta potential values is required for indication of stable nano-suspension [38, 39]. The zeta potential value for *K. alvarezii*/Cu@Cu_2O-NPs is –30.6 mV. So, this result clearly indicates that the produced NPs are less stable than *K. alvarezii*.

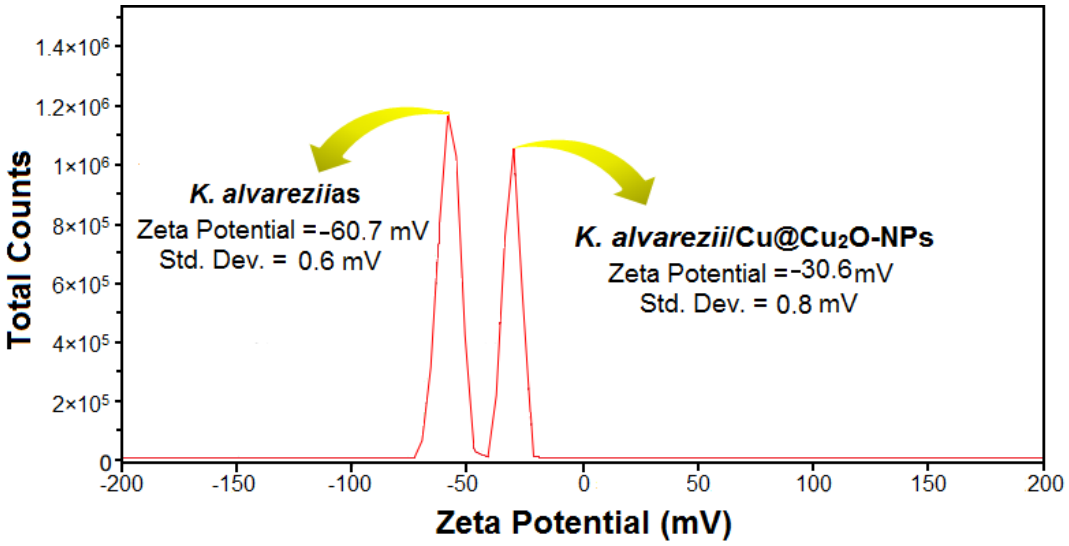

Figure 7. Zeta potential for *K. alvarezii* and *K. alvarezii*/Cu@Cu_2O core shell nanoparticles.

4. CONCLUSIONS

The Cu@Cu_2O core shell nanoparticles with mean size in the range of 53 nm and an fcc crystal structure had been successfully synthesized in *K. alvarezii* by a chemical method. The formation of core shell Cu@Cu_2O-NPs was confirmed in the UV-Vis absorption spectra, which showed the SPR band characteristics of Cu@Cu_2O-NPs at 590 and 390 nm. The XRD result shows that the ratio of Cu and Cu_2O-NPs in the sample is 75% and 25%, respectively. FT-IR spectrum suggested the core shell Cu@Cu_2O-NPs was capped by *K. alvarezii* and the stability of the *K. alvarezii*/Cu@Cu_2O-NPs was confirmed with the zeta potential measurements. Moreover, the morphology and structure of the NPs were investigated by TEM and AFM. This is a cheap, facile and environmental friendly method which leads to the formation of Cu@Cu_2O- NPs.

ACKNOWLEDGEMENTS
The authors are also grateful to the staff of the Department of Chemistry UPM and the Institute of Bioscience UPM for the technical assistance.

References

1. K. Iwasaki, T. Itoh, T. Yamamura. *Mater. Trans.* 46 (2005) 1368–1377.
2. K. Shameli, M.B. Ahmad, P. Shabanzadeh, J.E.A. Al-Mulla, A. Zamanian, Y. Abdollahi, S.D. Jazayeri, M. Eili, F. Azizi Jalilian, R.Z. Haroun. *Res. Chem. Intermed.* 40 (2014) 1313–1325.
3. K. Shameli, M.B. Ahmad, A. Zamanian, P. Sangpour, P. Shabanzadeh, Y. Abdollahi, M. Zargar, *Int. J. Nanomed.* 7 (2012) 5603–5610.
4. M.B. Ahmad, K. Shameli, W.M.Z. Wan Yunus, N.A. Ibrahim, A.A. Hamid, M. Zargar. *Res. J. Biol. Sci.* 4(9) (2009) 1032–1036.
5. K. Shameli, M.B. Ahmad, W.M.Z. Wan Yunus, N.A. Ibrahim, M. Jokar. *Proc. World Acad. Sci. Eng. Technol.* 64 (2010) 28–32.
6. K. Cattarin, M. Musianim. *Electrochim. Acta* 52 (2007) 2796–2805.
7. K. Park. D. Han, Y. Sung. *J. Power Sources* 163 (2006) 82–86.
8. K. Shameli, M.B. Ahmad, E.A.J. Al-Mulla, P. Shabanzadeh, S. Bagheri. *Res. Chem. Intermed.* (2013) 1–13. doi: 10.1007/s11164-013-1188-y
9. M.S. Usman, M.E.E. Zowalaty, K. Shameli, N. Zainuddin, M. Salama, N.A. Ibrahim. *Int. J. Nanomed.* 8 (2013) 4467–4479.
10. M.B. Ahmad, J.J. Lim, K. Shameli, N.A. Ibrahim, M.Y. Tay, B.W. Chieng. *Chem. Cent. J. 6*(101) (2012) 1–9.
11. J.M. Campelo, D. Luna, R. Luque, J.M. Marinas, A.A. Romero. *Chem. Sus. Chem. 2*(1) (2009) 18–45.
12. C. Dong, H. Cai, X. Zhang, C. Cao. *Physica. E* 57 (2013)12–20.
13. Z. Dongmei, S. Liguo, W. Yanjie, W. Cheng. *Prog. Chem.* 24 (2012) 1277–1293.
14. K. Bhatte, P. Tambade, K. Dhake, M. Bhanage. *Catal. Commun.* 11 (2010) 1233–1237.
15. R. Eluri, B. Paul, *Mater. Design.* 36 (2012) 13–23.
16. J. Wen, J. Li, S. Liu, Q. Chen. *Colloid Surfaces A* 373(1-3) (2011) 29–35.
17. J. Yun, K. Cho, B. Park, H. Kang, B. Ju, S. Kim. *Jpn. J. Appl. Phys.* 47 (2008) 5070–5075.
18. H. Zahang, U. Siegert, R. Liu, W. Bin Cai, *Nanoscale Res. Lett.* 4 (2009) 705–708.
19. A. Htain, C. Supab, C. Torranin. *Adv. Mat. Res.* 93 (2010) 83–86.
20. C. Kitchens, C. Roberts. *Ind. Eng. Chem. Res.* 43 (2004) 6070–6081

21. T.M.D. Dang, T.T.T. Le, E. Fribourg-Blanc, M.C. Dang. *Adv. Nat. Sci. Nanosci. Nanotechnol.* 2(025004) (2011) 1–7.
22. M. Nine, B. Munkhbayar, M. Rahman, H. Chung, H. Jeong. *Mater. Chem. Phy.* 141 (2013) 636–642.
23. S. Li, X. Guo, Y. Wang, A. Xie, F. Huang, Y. Shen, X. Wang. *Dalton T.* 40 (2011) 6745–6750.
24. L. Feng, C. Zhang, G. Gao, D. Cui. *Nano. Res. Lett.* 7(276) (2012) 1–10.
25. M. Sen, E. Erboz. *Food. Res. Int.* 43 (2010) 1361–1364.
26. S. Yallappa, J. Manjannan, M. Sindhe, N. Satyanarayan, S. Pramod, K. Nagaraja. *Spectrochimica Acta Part A: Molecular and Biomolecular Spectroscopy* 110 (2013) 108–115.
27. T. Ghodselahi, M.A. Vesaghi, A. Shafiekhani, A. Baghizadeh, M. Lameii. *Appl. Surf. Sci.* 255 (2008) 2730–2734.
28. A. Soon, M. Todorova, B. Delley, C. Stampfl. *Phys. Rev. B* 75(125420) (2007) 1–9.
29. K. Kumar, K. Ganesan, P. Subba-Rao. *Food Chem.* 107 (2008) 289–295.
30. A. Salgueiro, A. Daniel-da-Silva, A. Girao, P. Pinheiro, T. Trindade. *Chem. Eng. J.* 229 (2013) 276–284.
31. M.S. Usman, N. Ibrahim, K. Shameli, N. Zainuddin, W. Yunus, *Molecules* 17 (2012) 14928–14936.
32. K. Tian, C. Liu, H. Yang, X. Ren. *Colloid Surfaces A* 397 (2012) 12–15.
33. M. Valodkar, A. Pal, S. Thakore. *J. Alloy Compd*. 509 (2011) 523–528.
34. C. Cao, L. Xiao, L. Liu, H. Zhu, C. Chen, L. Gao. *Appl. Surf. Sci.* 271 (2013) 105-112.
35. M. Zargar, K. Shameli, G.R. Najafi, F. Farahani. *J. Ind. Eng. Chem.* (2014) 1–7. http://dx.doi.org/10.1016/j.jiec.2014.01.016.
36. S.; Balavandy, K.; Shameli, D.; Biak, Z. Zainl-Abidin, *Chem. Cent. J.* (2014) 1-10. doi: 10.1186/1752-153X-8-11.
37. A.M. Salgueiro, A.L. Daniel-da-Silva, A.V. Girão, P.C. Pinheiro, T. Trindade. *Chem. Eng. J.* 229 (2013) 276–284.
38. A. Wang, X. Li, Y. Zhao, W. Wu, J. Chen, H. Meng. *Powder Technol*. 261, (2014) 42–48.
39. K. Shameli, M.B. Ahmad, E.A.J. Al-Mulla, N.A. Ibrahim, P. Shabanzadeh, A. Rustaiyan, Y. Abdollahi, S. Bagheri, A. Sanaz, U.M. Sani, M. Zidan. *Molecules* 17(7) (2012) 8506–8517.